Replacement of calcium carbonate polymorphs by cerussite

YoungJae Kim[1,*], Bektur Abdilla[2], Ke Yuan[3], Vincent De Andrade[4,#], Neil C. Sturchio[2], Sang Soo Lee[1], Paul Fenter[1]

[1]Chemical Sciences and Engineering Division, Argonne National Laboratory, Lemont, Illinois 60439, United States

[2]Department of Earth Sciences, University of Delaware, Newark, Delaware 19716, United States

[3]Chemical Sciences Division, Oak Ridge National Laboratory, Oak Ridge, Tennessee 37831, United States

[4]Advanced Photon Source, Argonne National Laboratory, Lemont, Illinois 60439, United States

[#]Current Address: Sigray, Inc., 5750 Imhoff Drive, Suite I, Concord, California 94520, United States

* corresponding author; E-mail: youngjkm@anl.gov

Abstract

Calcium carbonate ($CaCO_3$) polymorphs, calcite, aragonite, and vaterite, serve as a major sink to retain various metal ions in the natural and engineered systems. Here, we visualize the systematic trends in reactivities of calcite, vaterite, and aragonite to Pb^{2+} dissolved in acidic aqueous solutions using in situ optical microscopy combined with ex situ scanning electron and transmission X-ray microscopies. All three polymorphs undergo pseudomorphic replacement by cerussite ($PbCO_3$) but with distinct differences in the evolution of their morphologies. The replacement of calcite and aragonite occurs through the formation of a pseudomorphic cerussite shell (typically 5-10 μm thick) followed by a slower inward propagation of reaction fronts through thin solution gap (~0.1 μm wide) between the shell and the $CaCO_3$ substrate. The replacement of vaterite is characterized by the formation of a thinner cerussite shell (≤ 1 μm thick) and a larger cavity between the shell and the host mineral. These systematic differences in cerussite morphology for the different $CaCO_3$ polymorphs are explained by the relative dissolution and precipitation rates of the reactants and products, coupled with the role of reactant transport through the cerussite product phase. We also find that the replacement of calcite by cerussite is found to be the slowest when all three polymorphs

coexisted. Our results provide mechanistic insights on the growth mode of cerussite on dissolving calcium carbonate and demonstrate these $CaCO_3$ polymorphs as promising substrate materials for removal and recycling of Pb from acidic polluted water and industrial effluents.

Keywords: Calcite, Aragonite, Vaterite, Cerussite, Mineral replacement, pore, Pb removal

Table of Contents/Abstract Graphics

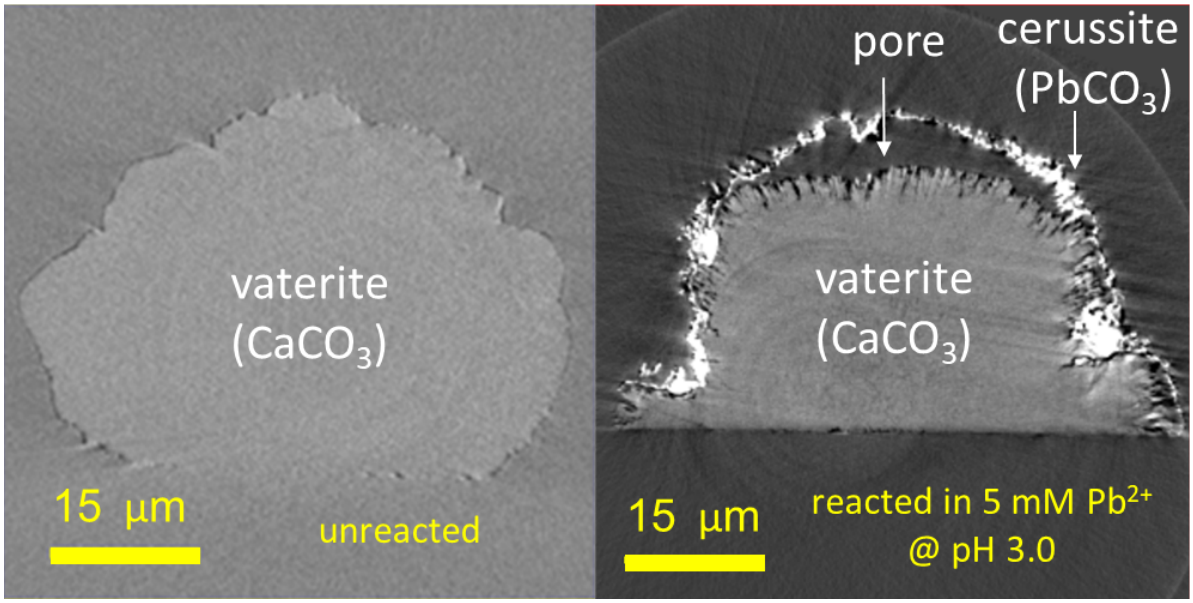

1. Introduction

Calcium carbonate ($CaCO_3$) occurs naturally in three crystalline polymorphs, calcite, aragonite, and vaterite. Calcite is the most stable phase of $CaCO_3$ in the ambient conditions and shallow waters of Earth's surface environments. Aragonite is commonly formed by biological processes in shells and coral skeletons in marine environments.[1-3] As the high pressure polymorph of $CaCO_3$, it is also observed in metamorphic rocks in subduction zones.[4] Vaterite is the least stable form of $CaCO_3$ and normally occurs as a metastable intermediate in the course of calcite nucleation[5, 6] or from biomineralization of carbon dioxide (CO_2).[7, 8] Besides their abundance in nature, the $CaCO_3$ polymorphs are of technological interest in the development of functional materials.[9-15] For example, calcium carbonate materials are used as fillers in paper and

adhesives, a major component in paints, base material for medical tablets, and sorbents for dissolved heavy metals.

Since the calcium carbonate polymorphs are highly reactive to dissolved ions, their mineral-water interfacial processes are critical in controlling the behavior of various metal ions in the natural and engineered systems. Among the three polymorphs, metal sequestration by calcite has been most widely studied and demonstrated to occur via mineral-water interfacial processes such as adsorption, precipitation, and incorporation.[16-25] Recently, there is an increasing awareness that the sequestration of dissolved heavy metals can occur via mineral replacement reactions.[26, 27] For example, calcite can be replaced by cerussite ($PbCO_3$) in acidic Pb^{2+}-containing solutions through coupled dissolution and precipitation with minimal changes in overall morphology.[28, 29] The distribution and growth rates of cerussite have previously been postulated to be controlled by spatial variations in both solution pH and local ion concentrations,[28-30] which determine the (local) saturation index of the precipitating phase. Furthermore, the cerussite product is highly porous, which facilitates transport of dissolved ions between the external solution and the substrate interfaces in the product phase.[29, 30]

Compared to calcite, less is known about the interaction of the other $CaCO_3$ polymorphs, aragonite and vaterite with dissolved Pb^{2+}. Although there is a consensus that Pb uptake by aragonite and vaterite can occur by mineral replacement,[31-35] which is similar to that by calcite, this is not yet supported by direct observation of the morphological relationship between the host phases and the secondary minerals. In addition, there are clear discrepancies among these studies. Gamsjager et al.[32] reported that Pb^{2+} uptake by aragonite occurs more rapidly and to a greater extent compared to that by calcite. In contrast, Di Lorenzo et al.[31] observed a lower reactivity of aragonite to Pb^{2+} than that of calcite. This lower reactivity appears resulting from surface passivation of aragonite by cerussite, which hinders further dissolution/precipitation at the interface. These previous studies highlight the need for systematic investigations of the crystallization of cerussite coupled with dissolution of the $CaCO_3$ polymorphs to assess the relative reactivity of these polymorphs in the presence of dissolved Pb^{2+}.

Here, we explore the reactivities of calcite, vaterite, and aragonite in the presence of dissolved Pb^{2+} to understand the mineralogical and morphological controls over the calcium carbonate-Pb^{2+} interaction. Calcium carbonate, in the form of single crystals or mixtures of calcium carbonate polymorphs, was subject to reactions with acidic Pb^{2+}-containing solutions. The morphological and chemical evolution of each polymorph, observed with optical microscopy, scanning electron microscopy (SEM), synchrotron X-ray nano-tomographic and fluorescence measurements, revealed that the growth mechanisms of the cerussite product (e.g., pseudomorphic replacement vs. cerussite shell formation) depended on the types of calcium carbonate polymorph. These different growth modes are postulated to be caused by the different solubilities and dissolution rates of the calcium carbonate polymorphs, providing new insights into the mechanisms of the replacement of carbonate minerals by cerussite. The results directly show differences in sorption mechanism among the individual polymorphs and provide a direct comparison of their uptake efficiencies, which will ultimately be important in designing the remediation strategy for Pb^{2+}- contaminated sites.

2. METHODS

Minerals and reagents

Calcium carbonate polymorphs were prepared in two ways. Most samples were synthesized on 0.8 × 0.8 cm^2 Kapton films or glass plates using the ammonium diffusion method.[36, 37] Calcite was the dominant product phase when grown at high Ca concentrations ($CaCl_2$ concentration ≥15 mM), while at intermediate and low Ca concentrations (≤10 mM $CaCl_2$), the mineral assemblages were mixtures of calcite, vaterite, and/or aragonite. Here, these mixture samples are denoted as vaterite/calcite and aragonite/vaterite/calcite to describe the mineral compositions. Additional powder specimens of calcium carbonate were prepared by crushing and sieving natural calcium carbonate minerals, including calcite (Chihuahua, Mexico) and aragonite (Ivanpah Mt., California, USA) crystals to obtain particle sizes ranging from 47 to 53 μm (similar to the crystals grown by the ammonium diffusion method). The prepared $CaCO_3$ samples were reacted with

acidic Pb^{2+}-containing solutions. Pb(II) stock solutions were prepared using Milli-Q® water (resistivity = 18.2 MΩ·cm; TOC < 5ppb) and lead nitrate ($Pb(NO_3)_2$, Sigma Aldrich; purity, 98-102 %).

Reaction Protocols

Operando observations of mineral replacement reactions were performed in situ using an in-house constructed fluid cell having an internal volume of 4.2 mL by sealing two transparent glass windows onto a cell body made of PEEK®.[29] An optical microscope equipped with a digital camera (Nikon Optiphot) and an image recording system was used in a transmission light mode. The reaction system in the fluid cell contained calcium carbonate minerals in contact with an input solution with 5 mM Pb(II) and an initial pH of 2.5–3.0, using a solid to solution ratio of 0.1–0.2 g/L. This initial solution was undersaturated with respect to calcite, resulting in dissolution of calcium carbonate minerals, which increased pH and (bi)carbonate concentration in solutions. The final solutions, after reaction for 16 to 24 hr, had the pH ranging from 4.2 to 4.5 and dissolved total carbonate concentrations of 1 to 2 mM, where the saturation index (SI) of cerussite ranged from −0.1 to 0.2 (because these solutions were not well-mixed, the cerussite saturation index was likely higher near the dissolving calcium carbonate, which therefore drove the local growth of the cerussite phase). Therefore, the increase of pH to values above 4 indicates that the solution chemistry evolved from the cerussite-undersaturated to saturated/supersaturated regimes. The morphological changes of $CaCO_3$ polymorphs were imaged periodically in real-time in the fluid cell by optical microscopy for reaction times up to 24 hr. After the reactions were completed, the samples were rinsed gently with ethanol, dried in air. The samples were then imaged using a Phenom scanning electron microscope (SEM) with energy dispersive X-ray spectroscopy (EDS) (Thermo Fisher Scientific).

High resolution X-ray fluorescence spectroscopy (XRF)

The reacted calcium carbonate minerals were analyzed using the synchrotron X-ray microprobe at beamline 13-ID-E at the Advanced Photon Source (APS), Argonne National Laboratory (ANL). X-ray fluorescence maps of Pb and Ca distributions on reacted calcium carbonates mounted on Kapton substrates were collected in a fly-scan raster mode using a 2 x 2 μm^2 beam size (5 x 5 μm^2 pixel size). Ca and Pb

fluorescence yields measured using Ca Ka1 and Pb La1 emission lines, respectively, were converted to ion concentrations by calibration with respect to thin film XRF reference samples (AXO Dresden) measured under the same experimental conditions.

Transmission X-ray Microscopy (TXM)

Synchrotron X-ray based nano-tomography measurements were performed at beamline 32-ID-C at the APS (ANL). The incident X-ray photon energy was 8 keV with a field of view of 51 × 51 μm^2. The sample was imaged in 721 projection directions spanning over ~180° of rotation angle with an exposure time of 0.5 or 1 s per image and a spatial resolution of 49 nm. Data reconstruction was processed using Tomopy.[38-40] The acquired images were further analyzed, and visualized in Fiji ImageJ.[41, 42]

RESULTS

Replacement reactions of individual $CaCO_3$ polymorphs by cerussite

Changes in external morphologies. Morphological changes of $CaCO_3$ polymorphs during reaction in acidic Pb-containing solutions were observed using an optical microscope (Figure 1) and SEM (Figure 2). Before the reaction, pristine calcite appeared as individual euhedral crystals, 30 to 80 μm in size (Figure 2a). Starting material vaterite commonly occurred in polycrystalline aggregates less than 150 μm in size having rounded surfaces (Figure 2b). Aragonite starting material also occurred in aggregates that had similar size to vaterite but with spiky surface features, distinctive from vaterite grains (Figure 2c).

Calcite crystals reacted in 5mM $[Pb^{2+}]_{initial}$ solution at pH 2.7 became smaller and less transparent with time in optical microscopy (Figure 1a). This variation in transparency likely resulted from changes of the

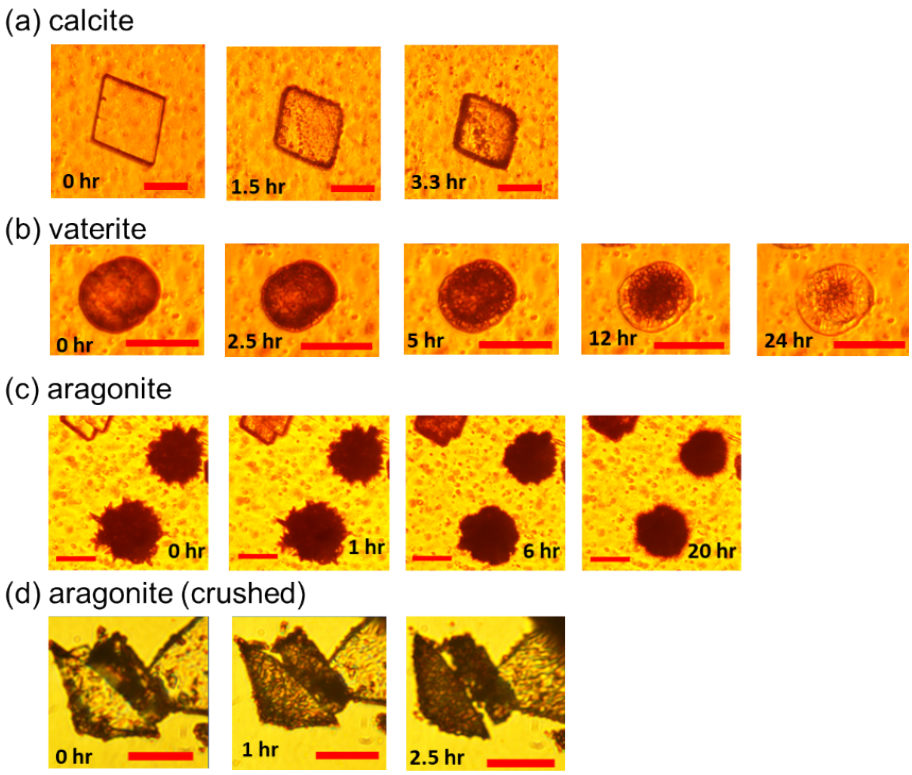

Figure 1. In situ optical micrograms of (a) calcite, (b) vaterite, and (c, d) aragonite in an acidic Pb^{2+} solution (i.e., initial pH 2.7 and 5 mM $Pb(NO_3)_2$) as a function of reaction time. The scale bars are 50 μm.

surface topography by the dissolution of the mineral substrate and the formation of cerussite (confirmed by XRD; Figure S.1b). Precipitation of cerussite occurred on the side surfaces of the crystal with respect to the Kapton support. Cerussite appeared as dark regions in optical microscope images (Figure 1a) and bright rod-shaped crystals in SEM images (Figure 2e). The small dotted patterns on the top surface of the crystal shown under optical microscope (Figure 1a) were mainly due to the dissolution of the calcite surface.[28]

Morphological changes of vaterite particles during reaction in the same solution composition ($[Pb^{2+}]_{initial}$ = 5mM; initial pH = 2.7) are shown in Figure 1b. After 2.5 hr of reaction, the particles became slightly darker presumably due to the dissolution of vaterite surfaces and precipitation of cerussite, the latter of which was confirmed by SEM (Figures 2f and j) and XRD (Figure S.1b). After 5 hr of reaction, the rim of

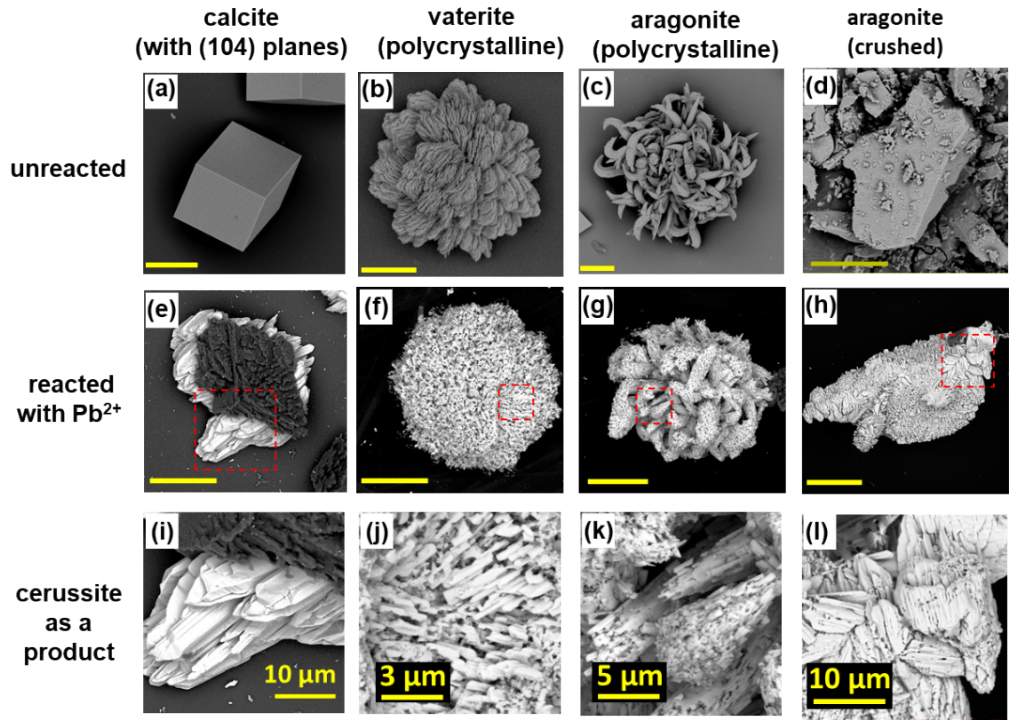

Figure 2. SEM images of calcite, vaterite, and aragonite (a-d) before and (e-l) after reaction with 5 mM $Pb(NO_3)_2$ at pH 2.7 for 16 hr. In (a to h), the scale bar is 30 µm. (i to l) Magnified images of the samples in (e to h) where cerussite products grow as tabular or reticulated crystals. In (a to l), the samples before and after the reaction are representative of each polymorph but are not identical particles.

the vaterite became optically translucent, and this translucent area propagated inward with time until it covered the entire vaterite surface (with respect to the projected area of the original particle) after 24 hr (Figure 1b).

Aragonite crystals reacted in the same solution composition ($[Pb^{2+}]_{initial}$ = 5mM; initial pH = 2.7) decreased in size and lost their spiny morphological features with time, indicating dissolution of the mineral substrate (Figure 1c). Little change in color was discernable for these particles by optical microscope. This is contrasted with observations of crushed aragonite particles, which changed from colorless (transparent)

to dark brown (opaque) within 2.5 hr of reaction with the same solution (Figure 1d). This color change indicates the formation of cerussite on the aragonite grains, which is confirmed by SEM (Figures 2k and 2l) and XRD (Figure S.1b).

Changes in internal structure. The changes in the internal structure of $CaCO_3$ minerals after the reaction with acidic Pb-containing solutions were examined using TXM (Figure 3). In these TXM images, the brightness is proportional to the density of the materials: lead carbonate, the heaviest phase in the system, appears brightest followed by calcium carbonate (intermediate) and air (darkest).

For reacted calcite and aragonite crystals, replacement by cerussite began at the external surfaces of the crystals, consistent with observations from optical microscopy. The cerussite layers on the substrates were typically ~5 to 10 μm thick. At the boundaries between the cerussite precipitate and the calcite substrates, pores were observed with a size of ~100 nm (Figures 3a and b), consistent with a previous study.[29]

The reacted vaterite specimens showed replacement structures that were distinct from those obtained

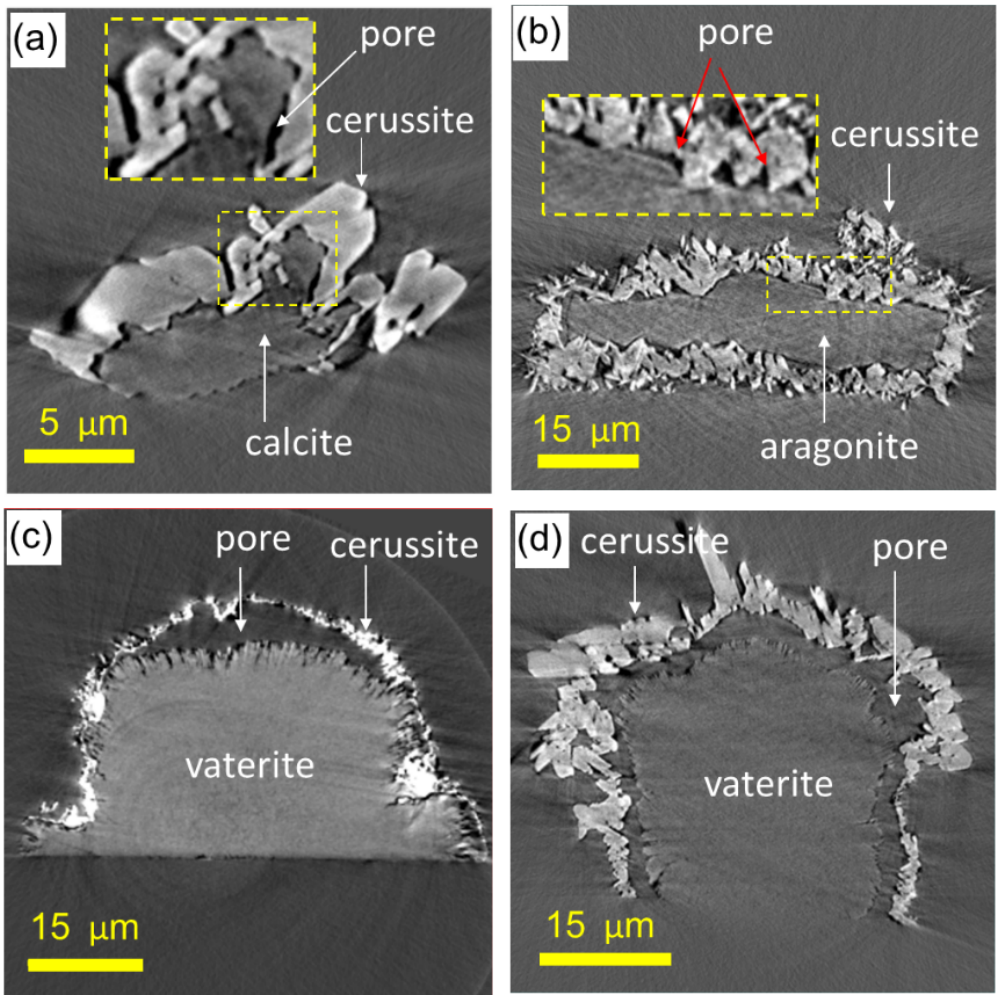

Figure 3. Nano-tomographic images of (a) calcite, (b) aragonite, and (c, d) vaterite crystals reacted with acidic Pb^{2+} solution (initial pH 2.7 and 5 mM $Pb(NO_3)_2$) for 6–16hr. Starting $CaCO_3$ materials were crushed calcite/aragonite and polycrystalline vaterite. Pores are found in reacted calcite and aragonite (a, b). In reacted vaterite, cerussite forms pseudomorphic shells over the outer part of the parent material

from calcite and aragonite. The replacement of vaterite was dominated by the formation of thin pseudomorphic cerussite shells (typically, ≤ 1 µm thick, Figure 3c). At the same time, the host vaterite continued to dissolve, resulting in the formation of large cavities separating the cerussite shells from the dissolving vaterite substrate. This internal structure of the reacted vaterite was consistent with the optical microscope observations (Figure 1b) where vaterite became initially darker and then increased in transparency. We postulate that the initial growth of precipitates was indicated by an increase in opaqueness while the subsequent formation of a large gap between the substrate and precipitation led to an increase in

transparency. In some cases, the extension of cerussite crystals into the aqueous solution was seen, indicating that the growth of the secondary cerussite occurred preferentially on the external surface of the shells (Figures 2i and 3d). This growth feature was more commonly observed around vaterite, especially when a large number of $CaCO_3$ particles was located in proximity to one another (i.e., in a high particle density per area). Similar replacement patterns have been seen previously for different systems, including lepidocrocite on calcite[43] (for calcite in acidic Fe^{2+} solutions) and bassanite on calcite[44] (for calcite in acidic SO_4^{2-} solutions).

Replacement reactions of $CaCO_3$ mixtures by cerussite

Mixtures of vaterite/calcite and aragonite/vaterite/calcite were reacted with acidic Pb^{2+} solution to determine relative reactivities of these $CaCO_3$ polymorphs with dissolved Pb^{2+}. The distributions of Ca and Pb measured by EDS and XRF showed that cerussite precipitation preferentially occurred on vaterite over calcite (Figure 4). This result is consistent with optical microscope observations of a vaterite/calcite mixture reacted with the same acidic Pb^{2+} solution (Figure S.2). When reacted simultaneously, vaterite particles showed significant changes in optical transparency whereas calcite particles showed little variations (Figure

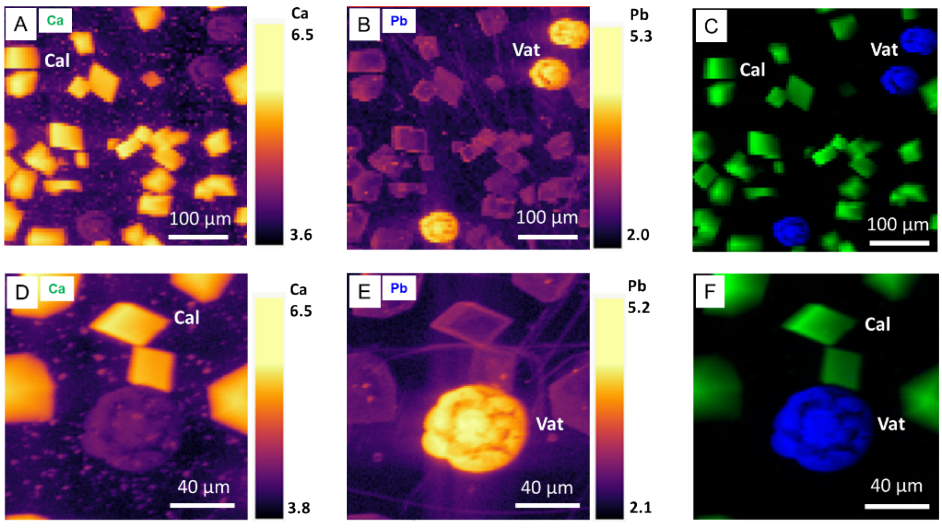

Figure 4. X-ray fluorescence maps of (A, D) Ca and (B, E) Pb and (C, F) two-colored maps of Ca (green) and Pb (blue) over the vaterite/calcite mixture reacted with 5 mM $Pb(NO_3)_2$ at pH 2.7 for 16 hr. The images in A to C and in D to F, respectively, show elemental maps over the same area. The angular particles are calcite and the rounded particles are vaterite. The color scale is in the unit of log (ng/cm^2).

S.2). The thickness of the cerussite shell around the dissolved vaterite grain was ~0.3 μm (estimated by dividing the Pb concentration per area (in units of 10^{-9} g/mm^2) by the density of cerussite, 6.58 g/cm^2 = 658 g/mm^2), which is in good agreement with the TXM result (Figure 3c). In turn, this result supports the interpretation that the main sorption mode of Pb on vaterite occurred as a mineral replacement reaction rather than surface adsorption. Aragonite was also found to preferentially retain Pb compared to calcite when these carbonate polymorphs coexisted in acidic Pb^{2+} containing solutions (Figure S.3).

Discussion

Chemical exchange between the calcium carbonate and the solution

The formation of pores between the dissolving calcium carbonate and the cerussite product was observed from the tomographic cross sections of calcium carbonate polymorphs reacted with acidic Pb^{2+} containing solution (Figures 3). During the replacement reactions, pores likely retained fluid that enabled chemical exchange among the dissolving carbonate mineral, the precipitating cerussite product, and the bulk solution. The main chemical reactions that are expected to occur during the replacement are

$$CaCO_{3(s)} + H^+ = Ca^{2+} + HCO_3^- \quad (1)$$

$$HCO_3^- + H^+ = H_2CO_3^0 \quad (2)$$

$$Pb^{2+} + HCO_3^- = PbCO_{3(s)} + H^+ \quad (3)$$

In acidic Pb^{2+}-containing solution, calcium carbonate minerals undergo a proton-mediated dissolution process, releasing Ca^{2+} and bicarbonate (HCO_3^-) (eq 1).[45] In an acidic bulk solution (with initial pH = 2.7 and final pH $\leq$ 4.5), bicarbonate can transform to the thermodynamically more stable carbonic acid ($H_2CO_{3(aq)}$) (eq 2), yet it is expected to be the dominant species near the carbonate mineral surface where pH is higher.[46] Within the pore space, therefore, it is likely that dissolved Pb^{2+} reacted with bicarbonate, leading to the formation of cerussite (eq 3). This interface-mediated dissolution/precipitation mechanism[26, 27] explains the observation that the overall morphologies of calcium carbonate polymorphs were preserved during their replacement by cerussite (Figure 2). In some cases (e.g., Figures 2i and 3d), the outward growth

of cerussite on the substrate occurred from dissolved carbonate species that were sourced externally from the bulk solution (for instance, through dissolution of neighboring calcium carbonate crystals).

Reactivity of calcium carbonates to dissolved Pb^{2+} under disequilibrium conditions

When calcite, aragonite, and vaterite coexisted, replacement reactions of $CaCO_3$ by Pb-carbonate occurred dominantly for vaterite and aragonite over calcite (Figures 4 and S.3). The different reactivities of these calcium carbonate minerals are likely due to their relative solubilities and dissolution rates. The solubility product constant, K_{sp} (= $a_{Ca^{2+}} \cdot a_{CO_3{}^{2+}}$, where a is the equilibrium activities of calcium and carbonate) at 25 ℃ and 1 atm is $10^{-8.48}$ for calcite, $10^{-8.34}$ for aragonite and $10^{-7.91}$ for vaterite,[47] showing that vaterite is more soluble than calcite and aragonite under ambient aqueous conditions. The vaterite and aragonite crystals examined in this study were polycrystalline (Figures 2b and c) whereas the calcite crystals were single euhedral crystals with (104) facets (Figure 2a). Therefore, the former likely had larger specific surface areas than the latter. Hence, one can expect that vaterite and aragonite dissolved faster than calcite. As a result, the local carbonate concentration near vaterite and aragonite crystals was expected to be higher than that near calcite crystals and thus cerussite was more likely to precipitate on vaterite and aragonite. The faster dissolution of vaterite and aragonite would have increased both solution pH and dissolved carbonate concentration, resulting in a decrease in the dissolution rate of neighboring calcite. Overall, the different reactivities of these $CaCO_3$ minerals revealed that the replacement reactions relied on the mass transport of dissolved carbonate and metal ions near the crystals, which was controlled by differences in the dissolution rates, solubilities, habits, and surface areas of the host minerals.

Reaction mechanisms of calcium carbonate replacement by cerussite

We have demonstrated that the outcome of the replacement reaction depends on the type and morphology of the initial calcium carbonate polymorphs with behavior ranging from nearly complete pseudomorphic mineral replacement to hollow cerussite shell formation. The primary control over these morphological differences appears to be the relative rates of calcium carbonate dissolution and product precipitation, which can be further altered or controlled by the local concentrations of chemical species that

are sourced from dissolving neighbors. Here, we use a conceptual model to demonstrate how the growth modes of cerussite on calcium carbonate polymorphs can be controlled by the balance between the dissolution and precipitation rates.

The nucleation and initial growth of cerussite occur spontaneously when fresh calcium carbonate crystals are reacted in acidic Pb^{2+} containing solutions (Figure 5a). Pore space between cerussite crystals allows diffusive flow of the acidic solution containing dissolved Pb^{2+} to the interface between the initial shell and the substrate, leading to further dissolution of $CaCO_3$ crystals and subsequent precipitation of cerussite. In the classical mineral-replacement model[26, 27], the precipitate growth and the substrate dissolution occur nearly at the same rates and the reaction front moves inward with little changes in its dimension[19, 20] (Figure 5b). In this mode, the dissolution and precipitation processes are spatially coupled and complete replacement of the substrate by the precipitate is possible. For example, our experimental conditions (i.e., solution pH, Pb concentration, and solid-to-solution ratio)[29] were chosen to satisfy these criteria for the replacement of calcite by cerussite (Figure 3a). When the substrate dissolution is faster than the precipitate growth, the gap between the substrate and the precipitate will be expanded, resulting in decoupling between the dissolution and precipitation processes (Figure 5c). Among the $CaCO_3$ polymorphs examined in this study, large separations between the host and secondary minerals were observed for vaterite reacted with dissolved Pb^{2+} (Figure 3c), presumably due to the faster dissolution rates of vaterite than those of calcite or aragonite (as described in the previous section).

We also observed a unique feature in which secondary cerussite crystals grew on the exterior of the pseudomorphic shells of some $CaCO_3$ polymorphs (Figure 3d). These observations were made for vaterite crystals when many of them were located closely together (i.e., in a high particle density). We expect that the external growth of cerussite is related to the fast dissolution of vaterite, which can lead to rapid increases in the local carbonate concentration and supersaturation of the solution with respect to cerussite. To drive external growth, the cerussite shell is required to be permeable to allow for the rapid transport of carbonate ions out of the shell (Figure 5d). Implicit in this model is the assumption that these reactions are transport

limited (including, diffusion of CO_3 away from and Pb towards the dissolving calcium carbonate, as mediated by the porosity of the cerussite shell). For example, limited growth of cerussite in the shell may result from a slow diffusion of dissolved Pb into the interior of the shell although the molecular origin that restricts the inward transport of the cation (while allowing outward diffusion of carbonate ions) is unclear. We also note the possibility that decoupling of the substrate dissolution from the precipitate growth (Figure 5d) may occur when the growth of the cerussite shell on the substrate occurs with carbonate species that are sourced externally (i.e., from the bulk solution, or from the local dissolution of neighboring carbonate crystals) as observed for vaterite crystals (Figure 3d and 5d).

Unlike the reaction for vaterite, the cerussite growth and $CaCO_3$ dissolution rates were found to be similar for calcite and aragonite (Figure 3a and b). The observed differences in cerussite morphology between these polymorphs likely originate from differences in the morphology of initial $CaCO_3$ polymorphs (e.g., calcite rhombs, crushed aragonite/calcite, and polycrystalline aragonite in Figure 2 and 3) and the ion permeability of porous cerussite shells, which would control chemical exchange between the pore and bulk solution. Overall, the differences in dissolution/precipitation patterns between $CaCO_3$ polymorphs reacted

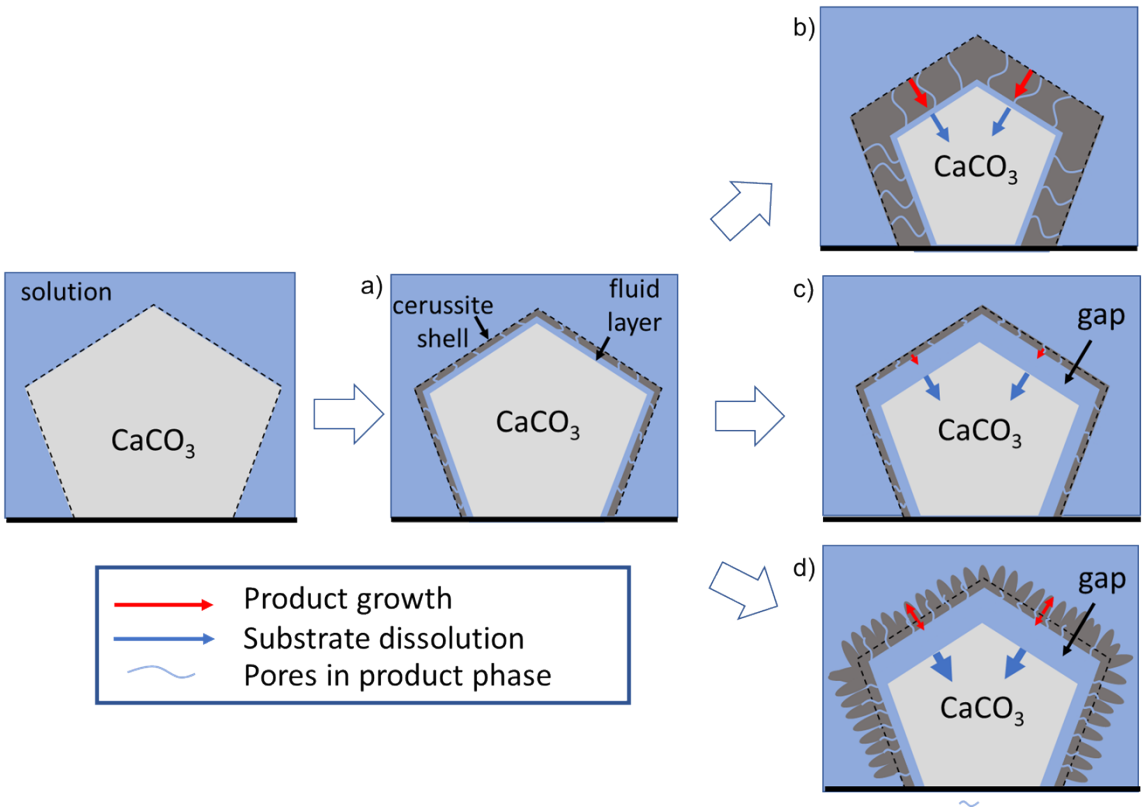

Figure 5. Proposed mechanisms for different growth modes of cerussite in calcium carbonate polymorphs. a) The formation of a cerussite shell from the reaction of carbonate minerals with acidic Pb^{2+} containing solution. The grain boundaries in the cerussite shell allow ion exchange between acidic solution and the carbonate substrate. This step may be followed by b) subsequent inward propagation of the thin solution layer via coupled dissolution/precipitation processes. Decoupling of the dissolution and precipitation processes can occur c) when the dissolution of the substrate is faster than the crystallization of the precipitate or d) when the local cerussite saturation index on the outside of the cerussite shell is sufficient to allow outward growth of cerussite on the shell. The behavior in d) can also occur when the reaction proceeds from carbonate species that are externally sourced from the bulk solution or the dissolution of neighboring particles.

with dissolved Pb^{2+} illustrate how the morphological evolution is controlled by the balance between the dissolution rate of the substrate and the precipitation rate of the product phase.

Conclusions

This study has established a mechanistic understanding of the replacement of $CaCO_3$ minerals by cerussite in acidic Pb^{2+}-containing aqueous solutions. The growth modes of cerussite on dissolving calcium carbonate crystals were observed to be sensitive to the choice of calcium carbonate polymorph, and the result of a delicate balance between dissolution and precipitation rates. The reactivities of calcium carbonate polymorphs are mineralogically and morphologically controlled. The replacement of calcite by cerussite was found to be slowest when all three polymorphs coexisted, which could be attributed to the different dissolution rates, solubilities, and morphologies among the polymorphs.

The present results provide a way to understand the reactivity of $CaCO_3$ with Pb^{2+} in natural environments. These support the concept that the dissolution of calcite, aragonite, and vaterite coupled with the precipitation of cerussite are significant sequestration mechanisms that occur under at acidic natural waters (pH 2.5 to 4.5; $[Pb^{2+}]_{initial}$ = 5 mM). Similar sorption mechanisms observed in the present study are expected to occur in environments where acidic Pb^{2+}-contaminated water interacts with carbonate-rich soils and rocks (e.g., mine tailings and acid mine drainage). While the Pb^{2+} containing fluid is transported through these carbonate-bearing media, the mobility of dissolved Pb^{2+} can be limited by precipitation of lead carbonates that are physically (and/or chemically) bound with the substrate of calcium carbonate. In environment where calcite and aragonite are in contact with mildly acidic to neutral Pb^{2+} containing solution (e.g., pH 5 to 7; $[Pb^{2+}]_{initial}$ = 0.05 to 5 mM)[31, 48], similar dissolution-precipitation processes might occur but in association with the formation of hydrocerussite as a main product. At more alkaline pH, such as when the solutions are at equilibrium with calcite and atmospheric CO_2 (i.e., at pH ~8.3), it is likely that the interaction of Pb^{2+} with $CaCO_3$ polymorphs will be distinct, occurring at lower concentrations (e.g.,

296 $[Pb^{2+}]_{initial}$ = 1 to 5 μM), both due to the formation of inner-sphere sorption complexes on calcite[17] and by
297 precipitation of Pb hydroxide.

298 The new understanding achieved in this study provides a mechanistic insight into the reaction
299 processes that might be leveraged for the remediation of Pb polluted environments. For remediation
300 purposes, calcite and aragonite can be sourced from natural rocks (e.g., limestone) and biogenic $CaCO_3$-
301 bearing materials such as egg/oyster shells. Vaterite can be formed via microbial mineralization[8] or
302 prepared by processing shell wastes.[33] Our studies demonstrate that these $CaCO_3$ polymorphs can be
303 promising substrate materials for Pb removal and potentially Pb recycling from acidic polluted water and
304 industrial effluents and that their relative reactivities could be important in designing related remediation
305 strategies. For example, rapid sequestration of Pb from contaminated water might be achieved by adding
306 vaterite and aragonite to induce precipitation on the exterior of pre-existing $CaCO_3$ grains. In contrast, the
307 use of complete replacement of calcite by cerussite might be more cost-effective for situations where
308 reaction capacity, rather than reaction rate, is the primary consideration, especially since calcite is the most
309 dominant $CaCO_3$ polymorph in natural systems. Systematic investigation of dissolution of calcium
310 carbonates coupled with precipitation of other forms of metal (e.g., Zn^{2+} and Cd^{2+}) carbonates will benefit
311 the development of alternative techniques for heavy metal sequestrations in geological and industrial
312 settings.

313

Acknowledgements

This work was supported by U.S. Department of Energy, Office of Science, Office of Basic Energy Sciences, Chemical Sciences, Geosciences, and Biosciences Division (Geochemistry Research Program) under Contracts DE-AC02-06CH11357 to UChicago Argonne, LLC as operator of Argonne National Laboratory. The X-ray data were collected at beamlines 13-ID-E (GeoSoilEnviroCARS) and 32-ID-C, Advanced Photon Source. We acknowledge the assistance of Drs. Tony Lanzirotti and Matt Newville at GeoSoilEnviroCARS. Use of the Advanced Photon Source was supported by the U.S. Department of Energy, Office of Science, Office of Basic Energy Sciences, under Contract DE-AC02-06CH11357 to UChicago Argonne, LLC as operator of Argonne National Laboratory. GeoSoilEnviroCARS is supported by the National Science Foundation – Earth Sciences (EAR – 1634415) and Department of Energy-GeoSciences (DE-FG02-94ER14466). The submitted manuscript has been created by UChicago Argonne, LLC, Operator of Argonne National Laboratory ("Argonne"). Argonne, a U.S. Department of Energy Office of Science laboratory, is operated under Contract No. DE-AC02-06CH11357. The U.S. Government retains for itself, and others acting on its behalf, a paid-up nonexclusive, irrevocable worldwide license in said article to reproduce, prepare derivative works, distribute copies to the public, and perform publicly and display publicly, by or on behalf of the Government.

Supporting Information description

X-ray diffraction patterns of aragonite, calcite, and vaterite/calcite mixture before and after reaction with acidic Pb^{2+}-containing solution; Variation in the morphology of a calcite/vaterite; in acidic Pb^{2+} solution; SEM images and energy dispersive X-ray spectroscopy measurement of a calcite/aragonite/vaterite mixture reacted in acidic Pb^{2+}-containing solution.

References

1. Checa, A. G.; Jiménez-López, C.; Rodríguez-Navarro, A.; Machado, J. P. Precipitation of aragonite by calcitic bivalves in Mg-enriched marine waters. *Mar. Biol.* **2007,** *150*, (5), 819-827.

2. Gillikin, D. P.; Lorrain, A.; Navez, J.; Taylor, J. W.; André, L.; Keppens, E.; Baeyens, W.; Dehairs, F. Strong biological controls on Sr/Ca ratios in aragonitic marine bivalve shells. *Geochem. Geophys. Geosyst.* **2005,** *6*, (5).

3. Keith, M.; Anderson, G.; Eichler, R. Carbon and oxygen isotopic composition of mollusk shells from marine and fresh-water environments. *Geochim. Cosmochim. Acta* **1964,** *28*, (10-11), 1757-1786.

4. Santillán, J.; Williams, Q. A high pressure X-ray diffraction study of aragonite and the post-aragonite phase transition in $CaCO_3$. *Am. Mineral.* **2004,** *89*, (8-9), 1348-1352.

5. Rodriguez-Blanco, J. D.; Shaw, S.; Benning, L. G. The kinetics and mechanisms of amorphous calcium carbonate (ACC) crystallization to calcite, via vaterite. *Nanoscale* **2011,** *3*, (1), 265-271.

6. Spanos, N.; Koutsoukos, P. G. The transformation of vaterite to calcite: effect of the conditions of the solutions in contact with the mineral phase. *J. Cryst. Growth* **1998,** *191*, (4), 783-790.

7. Li, H.; Yao, Q.-Z.; Wang, F.-P.; Huang, Y.-R.; Fu, S.-Q.; Zhou, G.-T. Insights into the formation mechanism of vaterite mediated by a deep-sea bacterium Shewanella piezotolerans WP3. *Geochim. Cosmochim. Acta* **2019,** *256*, 35-48.

8. Rodriguez-Navarro, C.; Jimenez-Lopez, C.; Rodriguez-Navarro, A.; Gonzalez-Muñoz, M. T.; Rodriguez-Gallego, M. Bacterially mediated mineralization of vaterite. *Geochim. Cosmochim. Acta* **2007,** *71*, (5), 1197-1213.

9. He, M.; Cho, B.-U.; Won, J. M. Effect of precipitated calcium carbonate—cellulose nanofibrils composite filler on paper properties. *Carbohydr. Polym.* **2016,** *136*, 820-825.

10. Jimoh, O. A.; Ariffin, K. S.; Hussin, H. B.; Temitope, A. E. Synthesis of precipitated calcium carbonate: a review. *Carbonates Evaporites* **2018,** *33*, (2), 331-346.

11. Karakaş, F.; Hassas, B. V.; Celik, M. S. Effect of precipitated calcium carbonate additions on waterborne paints at different pigment volume concentrations. *Prog. Org. Coat.* **2015,** *83*, 64-70.

12. Ok, Y. S.; Lee, S. S.; Jeon, W.-T.; Oh, S.-E.; Usman, A. R.; Moon, D. H. Application of eggshell waste for the immobilization of cadmium and lead in a contaminated soil. *Environ. Geochem. Health* **2011,** *33*, (1), 31-39.

13. Ok, Y. S.; Oh, S.-E.; Ahmad, M.; Hyun, S.; Kim, K.-R.; Moon, D. H.; Lee, S. S.; Lim, K. J.; Jeon, W.-T.; Yang, J. E. Effects of natural and calcined oyster shells on Cd and Pb immobilization in contaminated soils. *Environ. Earth Sci.* **2010,** *61*, (6), 1301-1308.

14. Poh, B.; Lee, P.; Chuah, S. Adhesion property of epoxidized natural rubber (ENR)-based adhesives containing calcium carbonate. *Express Polym. Lett.* **2008,** *2*, (6), 398-403.

15. Fausett, H.; Gayser, C.; Dash, A. K. Evaluation of quick disintegrating calcium carbonate tablets. *AAPS PharmSciTech* **2000,** *1*, (3), 37-43.

16. Callagon, E.; Fenter, P.; Nagy, K. L.; Sturchio, N. C. Incorporation of Pb at the calcite (104)–water interface. *Environ. Sci. Technol.* **2014,** *48*, (16), 9263-9269.

17. Elzinga, E. J.; Rouff, A. A.; Reeder, R. J. The long-term fate of Cu^{2+}, Zn^{2+}, and Pb^{2+} adsorption complexes at the calcite surface: An X-ray absorption spectroscopy study. *Geochim. Cosmochim. Acta* **2006,** *70*, (11), 2715-2725.

18. Rouff, A. A.; Elzinga, E. J.; Reeder, R. J.; Fisher, N. S. X-ray absorption spectroscopic evidence for the formation of Pb(II) inner-sphere adsorption complexes and precipitates at the calcite− water interface. *Environ. Sci. Technol.* **2004,** *38*, (6), 1700-1707.

19. Rouff, A. A.; Elzinga, E. J.; Reeder, R. J.; Fisher, N. S. The influence of pH on the kinetics, reversibility and mechanisms of Pb (II) sorption at the calcite-water interface. *Geochim. Cosmochim. Acta* **2005,** *69*, (22), 5173-5186.

20. Rouff, A. A.; Elzinga, E. J.; Reeder, R. J.; Fisher, N. S. The effect of aging and pH on Pb (II) sorption processes at the calcite− water interface. *Environ. Sci. Technol.* **2006,** *40*, (6), 1792-1798.

21. Rouff, A. A.; Reeder, R. J.; Fisher, N. S. Pb (II) sorption with calcite: A radiotracer study. *Aquat. Geochem.* **2002,** *8*, (4), 203-228.

22. Sturchio, N. C.; Chiarello, R. P.; Cheng, L.; Lyman, P. F.; Bedzyk, M. J.; Qian, Y.; You, H.; Yee, D.; Geissbuhler, P.; Sorensen, L. B. Lead adsorption at the calcite-water interface: Synchrotron X-ray standing wave and X-ray reflectivity studies. *Geochim. Cosmochim. Acta* **1997,** *61*, (2), 251-263.

23. Davis, J. A.; Fuller, C. C.; Cook, A. D. A model for trace metal sorption processes at the calcite surface: Adsorption of Cd^{2+} and subsequent solid solution formation. *Geochim. Cosmochim. Acta* **1987,** *51*, (6), 1477-1490.

24. Kang, C.-H.; Han, S.-H.; Shin, Y.; Oh, S. J.; So, J.-S. Bioremediation of Cd by microbially induced calcite precipitation. *Appl. Biochem. Biotechnol.* **2014,** *172*, (6), 2907-2915.

25. Zavarin, M.; Roberts, S.; Hakem, N.; Sawvel, A.; Kersting, A. Eu (III), Sm (III), Np (V), Pu (V), and Pu (IV) Sorption to Calcite. *Radiochim. Acta* **2005,** *93*, (2), 93-102.

26. Putnis, A. Mineral replacement reactions: from macroscopic observations to microscopic mechanisms. *Mineral. Mag.* **2002,** *66*, (5), 689-708.

27. Putnis, A. Mineral replacement reactions. In *Reviews in mineralogy and geochemistry*, 2009; Vol. 70, pp 87-124.

28. Yuan, K.; De Andrade, V.; Feng, Z.; Sturchio, N. C.; Lee, S. S.; Fenter, P. Pb^{2+}–Calcite Interactions under Far-from-Equilibrium Conditions: Formation of Micropyramids and Pseudomorphic Growth of Cerussite. *J. Phys. Chem. C* **2018,** *122*, (4), 2238-2247.

29. Yuan, K.; Lee, S. S.; De Andrade, V.; Sturchio, N. C.; Fenter, P. Replacement of calcite ($CaCO_3$) by cerussite ($PbCO_3$). *Environ. Sci. Technol.* **2016,** *50*, (23), 12984-12991.

30. Yuan, K.; Starchenko, V.; Lee, S. S.; De Andrade, V.; Gursoy, D.; Sturchio, N. C.; Fenter, P. Mapping three-dimensional dissolution rates of calcite microcrystals: Effects of surface curvature and dissolved metal ions. *ACS Earth Space Chem.* **2019,** *3*, (5), 833-843.

31. Di Lorenzo, F.; Ruiz-Agudo, C.; Churakov, S. V. The key effects of polymorphism during Pb^{II} uptake by calcite and aragonite. *CrystEngComm* **2019,** *21*, (41), 6145-6155.

32. Gamsjäger, H.; Fluch, A.; Swinehart, J. H. The effect of potential aqueous pollutants on the solubility of Pb^{+2} in cerussite—Calcite phase. *Monatsh. Chem.* **1984,** *115*, (3), 251-259.

33. Lin, P.-Y.; Wu, H.-M.; Hsieh, S.-L.; Li, J.-S.; Dong, C.; Chen, C.-W.; Hsieh, S. Preparation of vaterite calcium carbonate granules from discarded oyster shells as an adsorbent for heavy metal ions removal. *Chemosphere* **2020,** *254*, 126903.

34. Miyake, M.; Komarneni, S.; Roy, R. Immobilization of Pb^{2+}, Cd^{2+}, Sr^{2+} and Ba^{2+} ions using calcite and aragonite. *Cem. Concr. Res.* **1988,** *18*, (3), 485-490.

35. Munemoto, T.; Fukushi, K.; Kanzaki, Y.; Murakami, T. Redistribution of Pb during transformation of monohydrocalcite to aragonite. *Chem. Geol.* **2014,** *387*, 133-143.

36. Hu, Q.; Zhang, J.; Teng, H.; Becker, U. Growth process and crystallographic properties of ammonia-induced vaterite. *Am. Mineral.* **2012,** *97*, (8-9), 1437-1445.

37. Ihli, J.; Bots, P.; Kulak, A.; Benning, L. G.; Meldrum, F. C. Elucidating Mechanisms of Diffusion-Based Calcium Carbonate Synthesis Leads to Controlled Mesocrystal Formation. *Adv. Funct. Mater.* **2013,** *23*, (15), 1965-1973.

38. De Carlo, F.; Gürsoy, D.; Marone, F.; Rivers, M.; Parkinson, D. Y.; Khan, F.; Schwarz, N.; Vine, D. J.; Vogt, S.; Gleber, S.-C. Scientific data exchange: a schema for HDF5-based storage of raw and analyzed data. *J. Synchrotron Radiat.* **2014,** *21*, (6), 1224-1230.

39. Gürsoy, D.; De Carlo, F.; Xiao, X.; Jacobsen, C. TomoPy: a framework for the analysis of synchrotron tomographic data. *J. Synchrotron Radiat.* **2014,** *21*, (5), 1188-1193.

40. Pelt, D. M.; Gürsoy, D.; Palenstijn, W. J.; Sijbers, J.; De Carlo, F.; Batenburg, K. J. Integration of TomoPy and the ASTRA toolbox for advanced processing and reconstruction of tomographic synchrotron data. *J. Synchrotron Radiat.* **2016,** *23*, (3), 842-849.

41. Schindelin, J.; Arganda-Carreras, I.; Frise, E.; Kaynig, V.; Longair, M.; Pietzsch, T.; Preibisch, S.; Rueden, C.; Saalfeld, S.; Schmid, B. Fiji: an open-source platform for biological-image analysis. *Nat. Methods* **2012,** *9*, (7), 676-682.

42. Schmid, B.; Schindelin, J.; Cardona, A.; Longair, M.; Heisenberg, M. A high-level 3D visualization API for Java and ImageJ. *BMC bioinformatics* **2010,** *11*, (1), 1-7.

43. Yuan, K.; Lee, S. S.; Wang, J.; Sturchio, N. C.; Fenter, P. Templating Growth of a Pseudomorphic Lepidocrocite Microshell at the Calcite–Water Interface. *Chem. Mater.* **2018,** *30*, (3), 700-707.

44. Ruiz-Agudo, E.; Putnis, C. V.; Hövelmann, J.; Álvarez-Lloret, P.; Ibañez-Velasco, A.; Putnis, A. Experimental study of the replacement of calcite by calcium sulphates. *Geochim. Cosmochim. Acta* **2015,** *156*, 75-93.

45. Sjoeberg, E. L.; Rickard, D. T. Calcite dissolution kinetics: surface speciation and the origin of the variable pH dependence. *Chem. Geol.* **1984,** *42*, (1-4), 119-136.

46. Kawano, J.; Toyofuku, T.; Nishimura, K.; Ueda, A.; Nagai, Y.; Kawada, S.; Teng, H.; Nagai, T. Direct Two-Dimensional Time Series Observation of pH Distribution around Dissolving Calcium Carbonate Crystals in Aqueous Solution. *Cryst. Growth Des.* **2019,** *19*, (8), 4212-4217.

47. Plummer, L. N.; Busenberg, E. The solubilities of calcite, aragonite and vaterite in CO_2-H_2O solutions between 0 and 90 C, and an evaluation of the aqueous model for the system $CaCO_3$-CO_2-H_2O. *Geochim. Cosmochim. Acta* **1982,** *46*, (6), 1011-1040.

48. Godelitsas, A.; Astilleros, J. M.; Hallam, K.; Harissopoulos, S.; Putnis, A. Interaction of calcium carbonates with lead in aqueous solutions. *Environ. Sci. Technol.* **2003,** *37*, (15), 3351-3360.